Chemical Engineering Journal 165 (2010) 617–624

Contents lists available at ScienceDirect

Chemical Engineering Journal

journal homepage: www.elsevier.com/locate/cej

Neural model for the leaching of celestite in sodium carbonate solution

Deniz Bingol[a,*], Salih Aydogan[b], S. Sinan Gultekin[c]

[a] Kocaeli University, Chemistry Department, Umuttepe Campus, 41380 Kocaeli, Turkey
[b] Selçuk University, Mining Engineering Department, 42075 Konya, Turkey
[c] Selçuk University, Electrical & Electronics Engineering Department, 42075 Konya, Turkey

ARTICLE INFO

Article history:
Received 9 July 2010
Received in revised form 2 October 2010
Accepted 4 October 2010

Keywords:
Celestite
Strontium carbonate
Artificial neural network (ANN)
Extended delta-bar-delta (EDBD)

ABSTRACT

A neural model for computing the conversion kinetics of $SrSO_4$ to $SrCO_3$ was investigated in sodium carbonate solution, based on the multilayered perceptrons was presented. For this purpose the artificial neural network (ANN) method was used. The effects of stirring speed, temperature, mole ratio Na_2CO_3:$SrSO_4$ and particle size of the celestite on leaching kinetics were studied. The surface transformation of celestite to strontium carbonate in aqueous carbonate solutions was also supported by FT-IR spectroscopy. The conversion rate of celestite increases systematically with increasing temperature (up to 70 °C). Furthermore, the feasibility of replacing the SO_4^{2-} ions with CO_3^{2-} ions in the structure of the leached solid was also investigated by FT-IR. FT-IR results showed that the replacement of SO_4^{2-} ions in celestite by CO_3^{2-} ions in leaching conditions was nearly completed at 60 °C with a mole ratio Na_2CO_3:$SrSO_4$ = 4:1, solid to liquid = 5:500, −212+106 μm particle size, and 400 rpm stirring rate for an interval of 240 min. The first (up to 90 min) conversion result obtained was trained with an extended delta-bar-delta algorithm (EDBD), which is in the multilayered perceptrons and is a neural model structure. Results of other conversion times (90–240 min) results were predicted. Results predicted by the neural model were in very good agreement with the experimental results.

1. Introduction

Strontium sulfate occurs in nature as mineral celestite ($SrSO_4$), the principal ore of strontium. Strontium carbonate also occurs in nature as strontianite and can be mined from its deposit. It is, however, usually made from the mineral celestite. Celestite is converted to $SrCO_3$, the common commercial form of strontium. Production methods for conversion of celestite to $SrCO_3$ have been investigated using the black ash method (alternatively known as the calcining method) and the soda method (also known as direct conversion). In the black ash method, the celestite concentrate is calcined at the high temperature (generally over than 1000 °C), follows a leaching process of the resulting strontium sulfide with hot water, filtration to separate solid impurities and precipitation with sodium carbonate and/or carbon dioxide to produce the strontium carbonate [1,2]. In the direct conversion method, high-grade celestite ore is reacted with a solution containing a carbonate source that may be sodium carbonate and ammonium carbonate or ammonium bicarbonate to obtain directly low-grade strontium carbonate and sodium sulfate by-product [3–5]. It is reported that the black ash method produces chemical grade strontium carbonates that are 98% strontium carbonate and 2% byproducts and impurities. The soda ash method produces technical grade strontium carbonates, containing at least 97% strontium carbonate [6].

Strontium carbonate ($SrCO_3$) is not only the basic raw material for producing other strontium salts, but also an the important raw material for producing magnetic materials such as optic glass, cathode-ray tubes for color TVs, electromagnets and strontium ferrite. Moreover, it is used in medicine, chemical reagents, pigments, coating, ceramics, electrolytic zinc, sugar refining, and brilliant reds in fireworks and signal flares. Rapid development of the technology will continue to increase demand for strontium carbonate. Erdemoglu et al. [7] reported that investigations of conversion of celestite to strontium carbonate will continue because of high energy consumption in the black ash process during high temperature leaching and acid costs in the direct conversion process.

Celestite reacts with sodium carbonate, giving solid strontium carbonate and soluble sodium sulfate, according to

$$SrSO_{4(s)} + Na_2CO_{3(aq)} = SrCO_{3(s)} + Na_2SO_{4(aq)} \quad (1)$$

The reaction of ion replacement in mineral species has been the subject of many studies: Booth and Pollard [8] indicated that celestite was converted to pure strontium carbonate by dissolving in fused sodium chloride (not reacting with the ore) and adding sodium carbonate within less than 30 min at 840 °C with maximum conversion. Iwai and Toguri [3] proposed two reac-

* Corresponding author. Tel.: +90 2623032030; fax: +90 2623032003.
E-mail address: denizbingol1@gmail.com (D. Bingol).

1385-8947/$ – see front matter © 2010 Elsevier B.V. All rights reserved.
doi:10.1016/j.cej.2010.10.007

tion mechanisms for the leaching process from thermodynamic and kinetic points of view: an initial reaction, when a dense layer of $SrCO_3$ forms on the celestite surface, and a second reaction, when diffusion of the SO_4^{2-} ions through the $SrCO_3$ layer is rate determining. Castillejos et al. [4] reported that the leaching reaction of celestite with Na_2CO_3 solutions is topochemical, making it suitable for a shrinking core model that incorporates diffusion of CO_3^{2-} through the solution in the pores of the product layer as the rate-limiting step. Suárez-Orduña et al. [9] investigated structural characterization of converted strontianite ($SrCO_3$) crystals from $SrSO_4$ (celestite) under alkaline hydrothermal conditions by XRD, FT-IR, and SEM. Conversion of mineral $SrSO_4$ to $SrCO_3$ occurred by a typical dissolution-precipitation mechanism. Suárez-Orduña et al. [10] investigated the kinetics of the conversion of mineral celestite to strontianite under alkaline hydrothermal conditions and reported that the reaction rate was determined by the diffusion of sulfate ions through the porous layer of strontium carbonate formed on the celestite surface. Furthermore, details of the effect of the crystallographic structural changes associated with the replacement of SO_4^{2-} ions by monovalent (F^- and OH^-) ions in mineral $SrSO_4$ crystals [11] and chemical reactivity of the mineral celestite [12] in hydrothermal conditions have also been discussed. The pseudomorphic replacement of mineral barite ($BaSO_4$) crystals converted to barium carbonate under alkaline hydrothermal conditions was investigated because of the chemical and structural similarities of the mineral barite specie to celestite ($SrSO_4$) noted by Rendon-Angeles et al. [13]. Aydogan et al. [14] investigated dissolution kinetics of celestite ($SrSO_4$) in HCl solution with $BaCl_2$ to produce $SrCl_2$ in solution and showed that the dissolution of celestite is a process controlled by chemical reactions. Owusu and Litz [2] and Erdemoglu and Canbazoglu [1] contributed to the understanding of the chemistry of the black ash process. Recently Obut et al. [15] and Erdemoglu et al. [16] investigated direct conversion of celestite ($SrSO_4$) to strontium carbonate by mechanochemical processing in sodium carbonate solution to produce strontium carbonate.

In the present study, models based on artificial neural networks (ANNs) are presented for computing the conversion kinetics of celestite to $SrCO_3$ in Na_2CO_3 solution. Ability and adaptability to learn, generalizability, smaller information requirement, fast real-time operation, and ease of implementation features have made ANNs popular in the last few years [17–24]. Because of these fascinating features, ANNs are here used to model the relationship between leaching parameters and the obtained results.

2. Experimental

2.1. Materials

The celestite concentrate used in the study was obtained from Barit Maden T.A.Ş. Concentrator (Sivas, Turkey). The samples were wet sieved to obtain particle sizes in the ranges +212, −212+106, −106+75, −75+53 and −53 μm.

According to mineralogical and XRD analysis together with chemical analysis, celestite was the major mineral in the sample with minor gypsum ($CaSO_4{\cdot}2H_2O$) and trace barite ($BaSO_4$), while other minerals varied from 1.02% to 2.31% [14]. Chemical analyses of different size fractions of the sample are listed in Table 1.

2.2. Experimental procedure

The leaching experiments were conducted in a 1-l Pyrex beaker with a rubber cover in a thermostatically controlled water bath equipped with a thermometer. A Heidolph Mark RZR 2021 model mechanical stirrer with propeller was used for stirring. During setup of the experiments, solid content of the solution was held constant at 5:500 (w:v). Stirring speed varied from 200 to 600 rpm, temperature varied from 40 to 80 °C, and Na_2CO_3:$SrSO_4$ mole ratios varied from 1:1 to 4:1. The ratio of solid content of solution varied from 2.5:500 to 50:500. Particle size fractions used were +212, −212+106, −106+75, −75+53 and −53 μm. Results of converting celestite to strontium carbonate were calculated from dissolved sulfate values because the sulfate in the leach solution originated from the solubilized $SrSO_4$ content of celestite. For SO_4^{2-} analysis, leach solutions in the range 1–4 ml were taken from the reactor at various time intervals, and the sample solution was diluted with distilled water to 100 ml in a volumetric flask. Distilled water in the volume taken was immediately added to the leaching medium. These solutions were analyzed for sulfate using the turbid metric method with a Shimadzu UV-2450 UV–VIS spectrophotometer. Sulfate analyses were conducted to determine the amount of $SrSO_4$ passing to leach solution and thus to calculate stoichiometrically the amount of $SrCO_3$ in leach medium according to Eq. (1).

Table 1
Chemical analysis of the various size fractions of the celestite sample (wt.%).

Mineral	Particle size (μm)				
	+212	−212+106	−106+75	−75+53	−53
$SrSO_4$	94.38	95.69	96.67	97.32	97.24
$BaSO_4$	0.46	0.37	0.35	0.33	0.33
$CaSO_4{\cdot}2H_2O$	2.83	2.64	1.49	1.33	1.33
Others	2.31	1.30	1.49	1.02	1.10

The ultrasonic treatment was conducted with Ultrasons-H 3000838 P-Selecta model (J. P. Selecta, Barcelona, Spain) ultrasonic bath, which supplied a constant frequency of 40 kHz with temperature control.

Spectroscopic studies were conducted with a Bruker Tensor 27 model FT-IR spectrophotometer. After the leaching treatments, the reaction products were separated from the remaining solution, washed with distilled water, dried, weighed, and analyzed for FT-IR. According to FT-IR analysis, the solid phase is $SrCO_3$ in the final solid. The leaching experiments were also conducted in an ultrasonic bath.

3. Results and discussion

3.1. Dissolution of celestite

The general reaction of the direct conversion is given in Eq. (1), which goes to the right because of the difference between the solubility products of $SrSO_4$ ($K_{sp} = 2.8 \times 10^{-7}$) and $SrCO_3$ ($K_{sp} = 9.4 \times 10^{-10}$) [15]. According to the proposed reaction, diffusion of sulfate ions is controlled by the strontium carbonate formed on the celestite surface [3,4].

The experiments for replacement of SO_4^{2-} ions of mineral celestite with CO_3^{2-} ions in Na_2CO_3 solutions were directed by considering the effect on the exchange of SO_4^{2-} ions with CO_3^{2-} ions by the following factors: stirring speed, temperature, Na_2CO_3:$SrSO_4$ mole ratio, solid to liquid ratio, and particle size of celestite.

3.2. Effect of stirring speed

The effect of stirring speed on the conversion of celestite to strontium carbonate was investigated in the range of 200–600 rpm. Here, 5 g celestite was leached in 500 ml of Na_2CO_3 solution (4 times the stoichiometric amount) at 50 °C for −212+106 μm particle size by agitating. As seen in Fig. 1, speeds greater than 400 rpm did not affect the rate of conversion reaction.

Sufficient stirring was required to sustain particles in leaching solution with increasing dynamic effects; therefore, the stirring

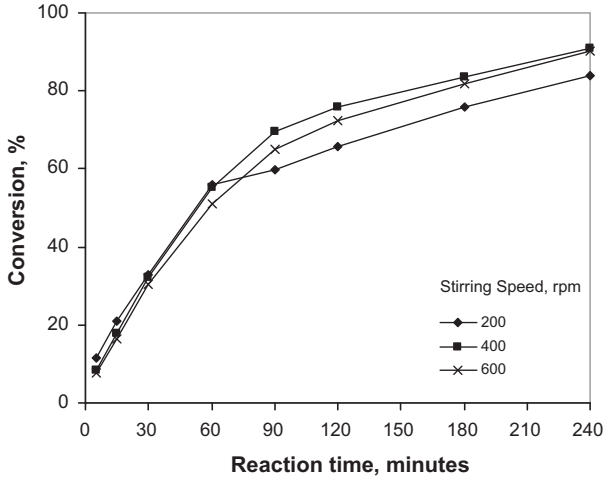

Fig. 1. Rate curves for the conversion of celestite to $SrCO_3$ at different stirring speeds (Na_2CO_3:$SrSO_4$ mole ratio: 4:1, solid to liquid ratio: 1:100 (w:v), weight of ore: 5 g, particle size: −212+106 μm, *T*: 50 °C).

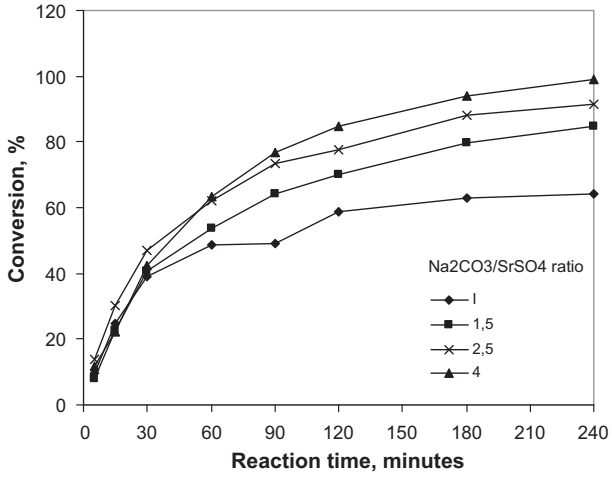

Fig. 3. Rate curves for the conversion of celestite to $SrCO_3$ with different amounts of Na_2CO_3 (solid to liquid ratio: 1:100 (w:v), weight of ore: 5 g, particle size: −212+106 μm, 400 rpm, *T*: 60 °C).

rate was kept constant at 400 rpm to investigate the effect of other parameters on the conversion.

3.3. Effect of temperature

Experiments to determine the effect of temperature on the dissolution of celestite were conducted in the temperature range of 40–80 °C. Fig. 2 shows the variation in conversion of celestite to strontium carbonate as a function of reaction time. As temperature increased, the conversion rate of celestite increased, up to 70 °C. After that, the conversion rate decreased. The conversion rate of celestite slowed down at 80 °C after 90 min.

Conversion under leaching conditions of celestite ($SrSO_4$) to $SrCO_3$ showed parabolic behaviour with respect to reaction times. At the beginning of the reaction (t < 90 min.), the reaction rate was faster because of a direct interaction between the surface of celestite and the reaction media. After that, formation of a product porous layer ($SrCO_3$) reduced the reaction rate [25].

Na_2CO_3 is a polybasic acid (H_2CO_3) ionized to give CO_3^{2-}, the main carbonating agent, and HCO_3^- ions. According to the dissolution equilibria of CO_2 in water given by Erdemoglu and Canbazoglu [1], the solubility of carbon dioxide decreases as temperature increases, enough to precipitate strontium ions in the form of $SrCO_3$ up to 75 °C. Temperatures greater than 75 °C cause the gasification of CO_3^{2-} ions as CO_2. Therefore, the conversion of celestite to strontium carbonate decreased at temperatures greater than 70 °C.

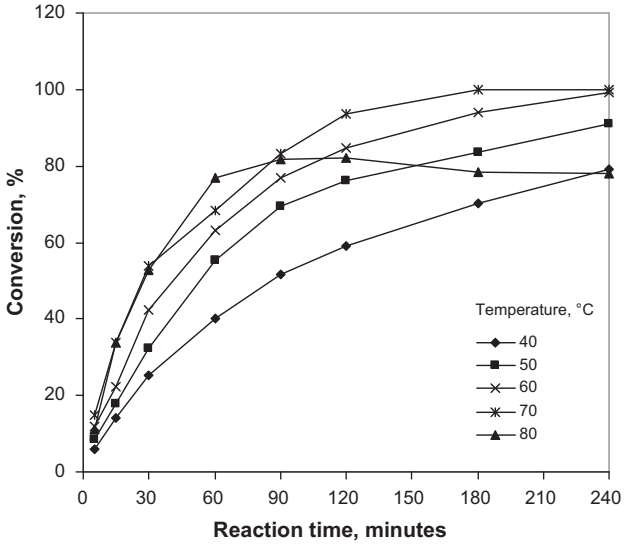

Fig. 2. Rate curves for the conversion of celestite to $SrCO_3$ at different leaching temperatures (Na_2CO_3:$SrSO_4$ mole ratio: 4:1, solid to liquid ratio: 1:100 (w:v), weight of ore: 5 g, particle size: −212+106 μm, 400 rpm).

3.4. Effect of the amount of sodium carbonate (Na_2CO_3:$SrSO_4$ mole ratio)

The effect of the quantity of sodium carbonate on conversion reaction was investigated for 1:1, 1:1.5, 1:2, 1:2.5, and 1:4 mole ratios of strontium sulfate: sodium carbonate at 60 °C. As shown in Fig. 3, the conversion of celestite to strontium carbonate was not complete after 240 min when the required stoichiometric amount of Na_2CO_3 was used. As the amount of Na_2CO_3 increased, the conversion of celestite to strontium carbonate increased. More than 90% of conversion occurred in 1:2.5 and 1:4 mole ratios.

Conversion occurs, dynamically as a result of direct contact between the surface of the celestite and the reaction media. Because of a high concentration of CO_3^{2-} ions, ion exchanges increase. Furthermore, the conversion of celestite to $SrCO_3$ increases with increasing the CO_3^{2-}:SO_4^{2-} ratio in the reaction interface. The conversion must be formed in excess of the stoichiometric amount required. The conversion of celestite to strontium carbonate tried with a stoichiometric of mole ratio of Na_2CO_3:$SrSO_4$ did not cause a significant change. Mole ratio is a decisive factor in the development of the reaction.

3.5. Effect of solid to liquid ratio

Fig. 4 shows the effect of solid to liquid ratio on the conversion of celestite in 500 ml solutions for 0.5:100, 1:100, 2:100, 4:100, 10:100 solid to liquid ratios (w:v). There was no variation in the conversion of celestite to strontium carbonate with a change in solid to liquid ratio up to a ratio of 2:100 as function of reaction time at 60 °C. It was observed that the change in this variable did not affect the development of the reaction up to 2:100, because no change was observed in the conversion grade due to an increase in the amount of solid used during leaching treatments. Then the rate of conversion decreased. This may be dependent on forming a porous layer around the unleached particles. Above the 4:100 ratio, sulfate analyses of leaching solutions were not conducted because of an interference effect of ions in leaching medium on sulfate analy-

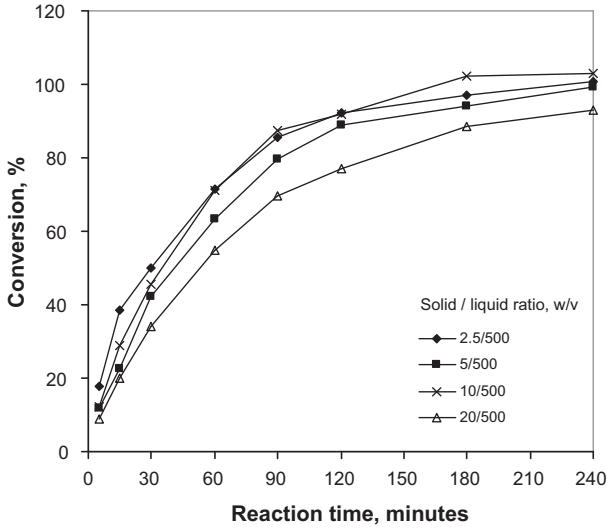

Fig. 4. Rate curves for the conversion of celestite to $SrCO_3$ at different solid to liquid ratios (Na_2CO_3:$SrSO_4$ mole ratio: 4:1, particle size: −212+106 μm, 400 rpm, *T*: 60 °C).

ses. Besides, as solid to liquid ratio increases, the separation of solid and liquid becomes more difficult.

3.6. Effect of particle size

Leaching reactions depend largely on particle size. Effect of particle size on the conversion of celestite to strontium carbonate was investigated by using particle size ranges of +212, −212+106, −106+75, −75+53 and −53 μm. Strontium carbonate recovery increased with decreasing particle size, as shown in Fig. 5.

It is clear that the conversion of celestite to $SrCO_3$ is rapid at the beginning. If the particle size decreases, the conversion is more rapid; however, the particle size effect decreases with increasing leaching time.

3.7. Effect of ultrasonic waves

Celestite was also converted to strontium carbonate by using an ultrasonic bath without agitation as a function of reaction time. Ultrasonic waves may be helpful in obtaining a more effective

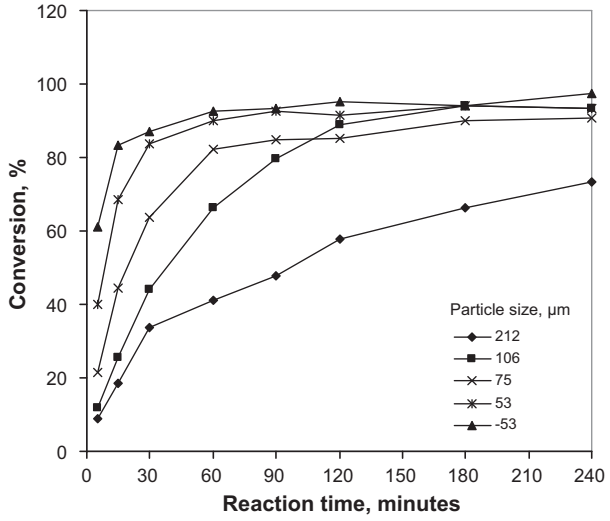

Fig. 5. Rate curves for the conversion of celestite to $SrCO_3$ with different particle size ranges (Na_2CO_3:$SrSO_4$ mole ratio: 4:1, solid to liquid ratio: 1:100 (w:v), weight of ore: 5 g, 400 rpm, *T*: 60 °C).

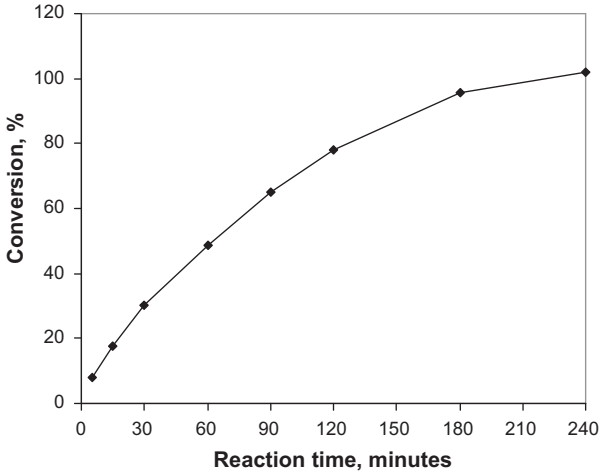

Fig. 6. Effect of ultrasonic treatment in the conversion of celestite to $SrCO_3$ (Na_2CO_3:$SrSO_4$ mole ratio: 4:1, solid to liquid ratio: 1:100 (w:v), weight of ore: 5 g, particle size: −212+106 μm, *T*: 60 °C).

solute transfer by changing solid structures and solvent fluidity. The high frequency (40 kHz) sound waves produce a cavitation effect which leads to the formation of millions of low pressure microscopic bubbles. Ultrasonic cavitations can effectively improve the thermal reaction equilibration [26]. However, as shown in Fig. 6, no significant change was observed in conversion rate of celestite by ultrasonic waves; conversion rate did not increase. For comparison, mechanical stirring is used after the celestite particles were placed into the carbonate solution with a stirring speed of 400 rpm differently than ultrasonic waves under the same conditions.

3.8. FT-IR studies

Conversion of the celestite surface to strontium carbonate was investigated by spectroscopy. Structural changes in the treated celestite could be observed in IR spectra. The spectroscopic results (Fig. 7) show IR spectra for celestite, with strontium carbonate formed by mechanical effect, and strontium carbonate formed by ultrasonic effect in leach solution, respectively.

In Fig. 7(a), the bands at 991 and 1081 cm^{-1} are characteristic of the sulfate group in celestite. The peaks at 698, 855 and 1770 cm^{-1} as well as the broad band at 1432 cm^{-1} seen in Fig. 7(b), define the carbonate group in formed strontium carbonate [10,11,25]. These stretching and bending modes were also reported in the celestite treated with ultrasonic effect at 698, 858, 1439, and 1771 cm^{-1} (Fig. 7(c)). These results demonstrate that the surface of celestite was transformed to strontium carbonate in the leaching conditions: Na_2CO_3:$SrSO_4$ mole ratio: 4:1, solid to liquid ratio: 1:100 (w:v), weight of ore: 5 g, particle size: −212+106 μm, *T*: 60 °C, t: 240 min, 400 rpm for (b), ultrasonic effect for (c). However, a peak remaining at 1070 cm^{-1}, corresponding to the SO_4^{2-} bending band, indicates the presence of a very small number of SO_4^{2-} ions, suggesting that unconverted raw $SrSO_4$ was still present in the reaction products even after 240 min of reaction. After the leaching treatments, it was observed that the $SrCO_3$ converted solid was almost completely different from the original mineral $SrSO_4$.

3.9. Artificial neural networks

ANNs are artificial systems, designed to mimic the human brain by extracting the relationships that underlie the data presented to them. They produce results very quickly because of their property of working in parallel to solve a specific problem. Thereby, they are quite effective in real-time problem solving. In the most gen-

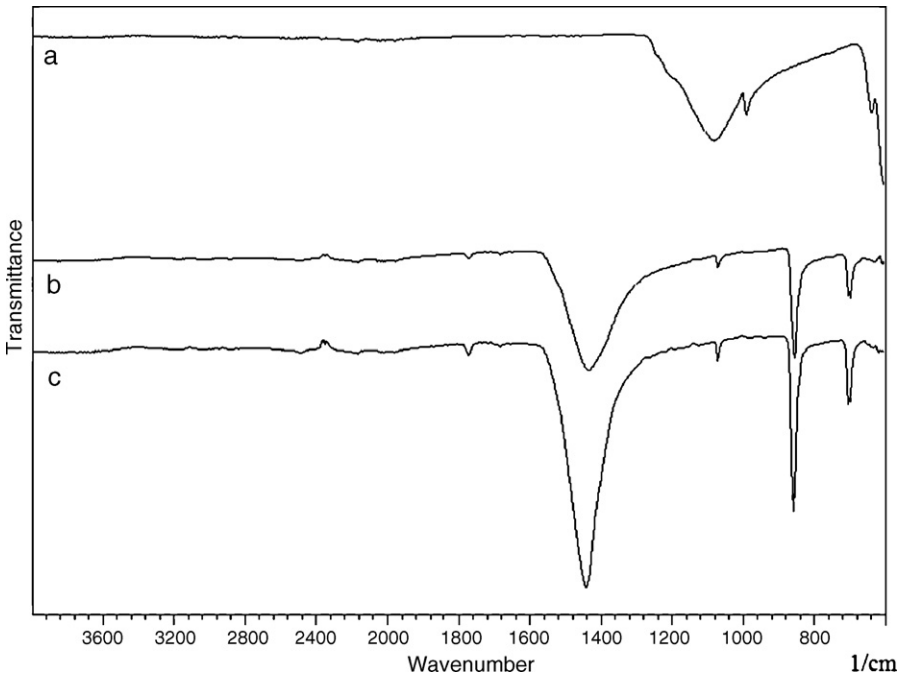

Fig. 7. FT-IR spectrums: (a) celestite ($SrSO_4$), (b) strontium carbonate ($SrCO_3$) formed mechanically (Na_2CO_3:$SrSO_4$ mole ratio: 4:1, solid to liquid ratio: 1:100 (w:v), weight of ore: 5 g, particle size: −212+106 μm, 400 rpm, *T*: 60 °C) and (c) strontium carbonate ($SrCO_3$) formed ultrasonically in sodium carbonate solutions (Na_2CO_3:$SrSO_4$ mole ratio: 4:1, solid to liquid ratio: 1:100 (w:v), weight of ore: 5 g, particle size: −212+106 μm, *T*: 60 °C).

eral sense, ANN can be assumed to be as a complex interconnected system of many neurons in the human brain or of simple processing elements connected artificially and with different impact levels. ANN is created by a means of interconnections of network neurons and usually organized into layers. Various ANN architectures are present [17,18,27].

3.9.1. Multilayered perceptrons

Multilayered perceptrons (MLPs) are the simplest and therefore most commonly used neural network architectures [17,18]. MLP consists of three layers: an input layer, an output layer, and an intermediate or hidden layer.

$$y_j = f(\Sigma w_{ji} x_i) \tag{2}$$

Neurons in the input layer act only as buffers for distributing input signals x_i to neurons in the hidden layer. Each neuron j in the hidden layer sums up its input signals x_i after weighting them with strengths of the respective connections w_{ji} from the input layer and computes its output y_j as a function f of the sum, viz., f can be a simple threshold function, a sigmoid, or a hyperbolic tangent function. The output of neurons in the output layer is computed similarly.

Training a network consists of adjusting weights of the network using various the different learning algorithms such as back propagation, quick prop, genetic algorithm, delta-bar-delta (DBD), extended delta-bar-delta (EDBD), etc. A learning algorithm gives the change $\Delta w_{ji}(k)$ in the weight of a connection between neurons i and j. In the following section, only one learning algorithm (EDBD) was used in this paper and is briefly explained.

3.9.2. Extended delta-bar-delta algorithm

The EDBD algorithm is an extension of the DBD and based on decreasing the training time for MLPs [24]. In this algorithm, the changes in weights are calculated as

$$\Delta w(k+1) = \alpha(k)\delta(k) + \mu(k)\Delta w(k) \tag{3}$$

and the weights are then found as

$$w(k+1) = w(k) + \Delta w(k+1) \tag{4}$$

In Eq. (3), $\alpha(k)$ and $\mu(k)$ are the learning and momentum coefficients, respectively. The learning coefficient change is given as

$$\Delta\alpha(k) = \begin{cases} \kappa_\alpha \exp(-\gamma_\alpha \left|\bar{\delta}(k)\right|), & \text{if } \bar{\delta}(k-1)\,\delta(k) > 0 \\ -\varphi_\alpha\, \alpha(k), & \text{if } \bar{\delta}(k-1)\delta(k) < 0 \\ 0, & \text{otherwise} \end{cases} \tag{5}$$

where κ_α is the constant learning coefficient scale factor, exp is the exponential function, φ_α is the constant learning coefficient decrement factor, and γ_α is the constant learning coefficient exponential factor. The momentum coefficient change is also written as

$$\Delta\mu(k) = \begin{cases} \kappa_\mu \exp(-\gamma_\mu \left|\bar{\delta}(k)\right|), & \text{if } \bar{\delta}(k-1)\,\delta(k) > 0 \\ -\varphi_\mu\, \mu(k), & \text{if } \bar{\delta}(k-1)\delta(k) < 0 \\ 0, & \text{otherwise} \end{cases} \tag{6}$$

where κ_μ is the constant momentum coefficient scale factor, φ_μ is the constant momentum coefficient decrement factor, and γ_μ is the constant momentum coefficient exponential factor.

In order to take a step further to prevent wild jumps and oscillations in the weight space, ceilings are placed on the individual connection learning and momentum coefficients. For this, $\alpha(k) \le \alpha_{\max}$, $\mu(k) \le \mu_{\max}$ must be for all connections, where $\alpha_{\max}$ is the upper bound on the learning coefficient, and $\mu_{\max}$ is the upper bound on the momentum coefficient.

Finally, after each epoch presentation of training tuples, the accumulated error is evaluated. If the error $E(k)$ is less than the previous minimum error, the weights are saved as the current best. A recovery tolerance parameter λ controls this phase. Specifically, if the current error exceeds the minimum previous error such that $E(k) > E_{\min}\lambda$ all connection weights revert to the stored best set of weights in memory. Further, both coefficients are decreased to begin the recovery.

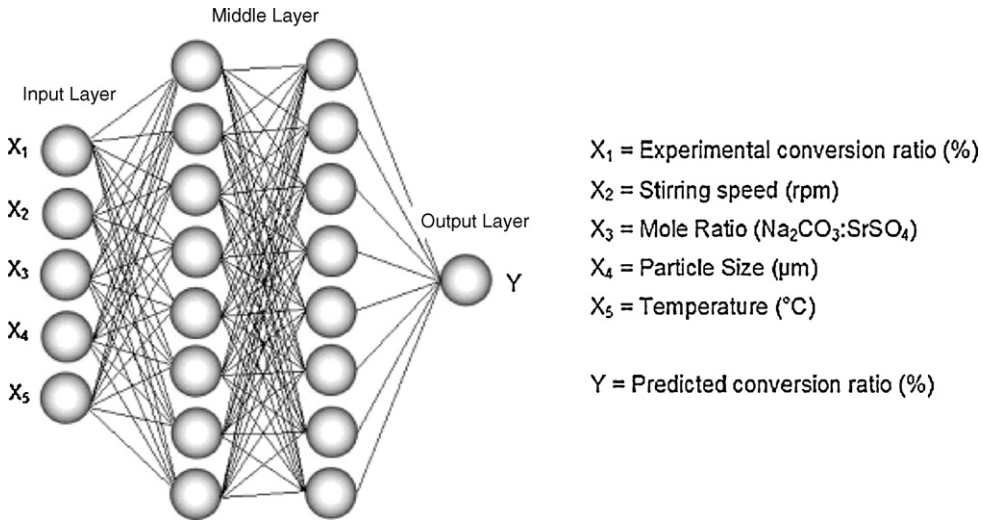

Fig. 8. The ANN model for predicted conversion (%).

3.9.3. Conversion prediction of $SrSO_4$ to $SrCO_3$ in sodium carbonate solution with neural network model

In recent years, artificial intelligence applications were applied in several areas. Especially, they have been found in the areas of metallurgy and leaching applications [28–33]. ANNs were adapted for prediction of the conversion of $SrSO_4$ to $SrCO_3$ in sodium carbonate solution. A neural model used to predict of conversion of $SrSO_4$ to $SrCO_3$ ratio is shown in Fig. 8.

MLP is trained with the use of EDBD algorithm. For the neural model, the inputs are experimental conversion (%), stirring speed (rpm), mole ratio (Na_2CO_3:$SrSO_4$), particle size (μm) and temperature (°C); output is the measured conversion of $SrSO_4$ to $SrCO_3$ ratio. In the MLP structure, input layer has the linear transfer function and the hidden and output layers have the tangent hyperbolic function. In the EDBD, the Gaussian function was used.

Training an ANN to predict with the use of a learning algorithm (EDBD) involves presenting different sets in sequence (experimental conversion (%), stirring speed (rpm), mole ratio (Na_2CO_3:$SrSO_4$), particle size (μm), and temperature (°C)) and corresponding measured values of conversion $SrSO_4$ to $SrCO_3$ ratio.

Differences between the target output predicted conversion ratio and the actual output of the ANN are evaluated by the EDBD. Adaptation occurs after the presentation of each set (experimental conversion (%), stirring speed (rpm), mole ratio (Na_2CO_3:$SrSO_4$), particle size (μm) and temperature (°C) predicted conversion) until the calculation accuracy of the network is deemed satisfactory according to some criterion (for example, when the error between predicted and actual output for the entire training set falls below a given threshold) or the maximum allowable number of epochs is reached.

The training and test datasets used for predicting conversion ratio were obtained from the experimental work and are given in Table 2. The 80 data sets in Table 2 were used to train the network, and 48 shown in boldface type were used for testing.

Table 2
Comparison of experimental and calculated conversion ratio by using a neural model of leaching of celestite in sodium carbonate solution.

Leaching time (min)	Stirring speed (rpm)	Mole ratio (Na_2CO_3:$SrSO_4$)	Particle size (μm)	Temperature (°C)	Experimental conversion ratio (%)	Predicted conversion ratio (%)
5	200	4	159	50	11.38	11.36
15	200	4	159	50	21.08	20.98
30	200	4	159	50	32.84	34.15
60	200	4	159	50	55.77	51.72
90	200	4	159	50	59.69	62.28
120	**200**	**4**	**159**	**50**	**65.62**	**69.21**
180	**200**	**4**	**159**	**50**	**75.85**	**77.6**
240	**200**	**4**	**159**	**50**	**83.92**	**82.38**
5	400	4	159	70	14.94	14.94
15	400	4	159	70	33.99	34.07
30	400	4	159	70	53.83	53.72
60	400	4	159	70	68.45	71.31
90	400	4	159	70	83.11	79.52
120	**400**	**4**	**159**	**70**	**93.62**	**84.84**
180	**400**	**4**	**159**	**70**	**99.94**	**92.26**
240	**400**	**4**	**159**	**70**	**99.94**	**97.77**
5	400	4	25	60	61.21	62.24
15	400	4	25	60	83.41	81.98
30	400	4	25	60	87.13	88.22
60	400	4	25	60	92.53	91.64
90	400	4	25	60	93.27	92.91
120	**400**	**4**	**25**	**60**	**95.1**	**93.6**
180	**400**	**4**	**25**	**60**	**94.2**	**94.34**
240	**400**	**4**	**25**	**60**	**97.36**	**94.75**

The test data are shown in bold characters, others are training data.

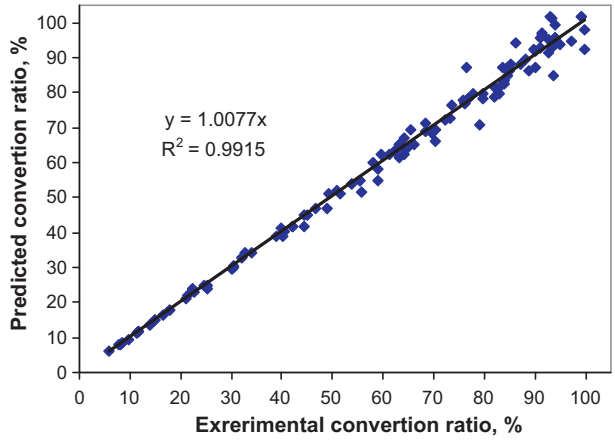

Fig. 9. Experimental conversion ratio results vs. obtained conversion ratio.

After several trials, it was found that networks of two hidden layers achieved the task with great accuracy. The iteration number was 25 million and numbers of neurons in the hidden layers were 8 and 8.

A set of random values distributed uniformly between −0.1 and +0.1 was used to initialize the weights of the networks, whereas tuples were scaled between −1.0 and +1.0 for inputs and −0.8 and +0.8 for outputs before training. Random and sequential training strategies were followed. The parameters of the network are:

$$\text{EDBD}, \quad \kappa_\alpha = 0.095, \quad \kappa_\mu = 0.01, \quad \gamma_\mu = 0.0, \quad \gamma_\alpha = 0.0,$$
$$\phi_\mu = 0.01, \quad \phi_\alpha = 0.1, \quad \theta = 0.7, \quad \lambda = 50;$$

The experimental conversion ratio results vs. conversion ratio obtained by using the neural model for leaching of celestite in sodium carbonate solution was drawn (Fig. 9), and the correlation coefficient (R^2) was calculated as 0.9915. As seen in Fig. 9, the performance of the neural model is in good agreement with experimental results.

Used for training, "predicted conversion ratio (%)" (training output) approach to the arithmetic average error 0.8581, 0.9114 error rate was calculated as the standard deviation. Used for testing, "predicted conversion ratio (%)" (testing out) approach to error arithmetic average of 3.2209, the error rate of the standard deviation was found to be 2.5827.

4. Conclusions

In the present study, the conversion of celestite in Na_2CO_3 solutions under leaching conditions was investigated over a broad range of experimental conditions. The effects of variables of temperature, solid to liquid ratio, particle size, stirring rate, and molar ratio Na_2CO_3:$SrSO_4$ were studied. It was found that the conversion rate of celestite to strontium carbonate increased systematically with increasing temperature (up to 70 °C). In addition, FT-IR results showed that the replacement of SO_4^{2-} ions in celestite by CO_3^{2-} ions under leaching conditions was nearly completed at 60 °C. Based on experimental observations, a mechanism for the conversion of celestite (fraction of Sr leached or converted to carbonate) under leaching conditions is proposed.

The obtained predicted results of the neural model were in very good agreement with the experimental results (R^2 = 0.9915). In addition, the test output data to the estimated standard deviation for 48 data was found to be 2.5827. This value means that the ANN model is quite well-educated and estimated.

The good agreement between the experimental values and computed conversion ratio values supports the validity of the neural model. A distinct advantage of neural computation is that, after proper training, a neural network completely bypasses the repeated use of complex iterative processes for new cases presented to it. For engineering applications, the simple models are very usable. Thus the neural model given in this work can also be used for many engineering applications and purposes.

References

[1] M. Erdemoglu, M. Canbazoglu, The leaching of SrS with water and the precipitation of $SrCO_3$ from leach solution by different carbonating agents, Hydrometallurgy 49 (1998) 135–150.
[2] G. Owusu, J.E. Litz, Water leaching of SrS and precipitation of $SrCO_3$ using carbon dioxide as the precipitating agent, Hydrometallurgy 57 (2000) 23–29.
[3] M. Iwai, J.M. Toguri, The leaching of celestite in sodium-carbonate solution, Hydrometallurgy 22 (1989) 87–100.
[4] E.A.H. Castillejos, F.P. delaCruz, A. Uribe, The direct conversion of celestite to strontium carbonate in sodium carbonate aqueous media, Hydrometallurgy 40 (1996) 207–222.
[5] Z. Cheng, T. Jiang, Production of strontium carbonate by ammonium bicarbonate method without remaining barium, Huadong Huagang Xueyuan Xuebao 18 (1992) 723–728.
[6] J.A. Ober, Strontium. U.S. Geological Survey Minerals Yearbook, 2001, pp. 74.1–74.4 http://minerals.usgs.gov/minerals/pubs/commodity/strontium/srmyb01.pdf.
[7] M. Erdemoglu, S. Aydogan, E. Gock, Effects of intensive grinding on the dissolution of celestite in acidic chloride medium, Miner. Eng. 22 (2009) 14–24.
[8] H.S. Booth, E.F. Pollard, Conversion of celestite to strontium carbonate, Ind. Eng. Chem. 40 (1948) 1986–1988.
[9] R. Suárez-Orduña, J.C. Rendón-Angeles, Z. Matamoros-Veloza, K. Yanagisawa, Exchange of SO_4^{2-} ions with F^- ions in mineral celestite under hydrothermal conditions, Solid State Ionics 172 (2004) 393–396.
[10] R. Suárez-Orduña, J.C. Rendón-Angeles, K. Yanagisawa, Kinetic study of the conversion of mineral celestite to strontianite under alkaline hydrothermal conditions, Int. J. Miner. Process. 83 (2007) 12–18.
[11] R. Suárez-Orduña, J.C. Rendón-Angeles, L. López-Cuevas, K. Yanagisawa, The conversion of mineral celestite to strontianite under alkaline hydrothermal conditions, J. Phys.: Condens. Matter 16 (2004) S1331–S1344.
[12] J.C. Rendon-Angeles, M.I. Pech-Canul, J. Lopez-Cuevas, Z. Matamoros-Veloza, K. Yanagisawa, Differences on the conversion of celestite in solutions bearing monovalent ions under hydrothermal conditions, J. Solid State Chem. 179 (2006) 3645–3652.
[13] J.C. Rendon-Angeles, Z. Matamoros-Veloza, J. Lopez-Cuevas, M.I. Pech-Canul, K. Yanagisawa, Stability and direct conversion of mineral barite crystals in carbonated hydrothermal fluids, J. Mater. Sci. 43 (2008) 2189–2197.
[14] S. Aydogan, M. Erdemoglu, A. Aras, G. Ucar, A. Ozkan, Dissolution kinetics of celestite ($SrSO_4$) in HCl solution with $BaCl_2$, Hydrometallurgy 84 (2006) 239–246.
[15] A. Obut, P. Baláž, I. Girgin, Direct mechanochemical conversion of celestite to $SrCO_3$, Miner. Eng. 19 (2006) 1185–1190.
[16] M. Erdemoglu, S. Aydogan, M. Canbazoglu, A kinetic study on the conversion of celestite ($SrSO_4$) to $SrCO_3$ by mechanochemical processing, Hydrometallurgy 86 (1–2) (2007) 1–5.
[17] D.E. Rumelhart, J.L. McClelland, Parallel Distributed Processing, The MIT Press, Cambridge, 1986.
[18] S. Haykin, Neural Networks: A Comprehensive Foundation, Macmillan College Publishing Company, NY, 1994.
[19] K. Guney, S. Gultekin, S. Sagıroglu, Design of Circular Microstrip Antennas Using Artificial Neural Networks, in: Proc. of 10th Turkish Symposium on Artificial Intelligence and Neural Networks (TAINN'2001), Gazimagusa, Turkish Republic of Northern Cyprus, s. 12–21, June, 2001.
[20] Q.J. Zhang, K.C. Gupta, Neural Networks for RF and Microwave Design, Artech House, Boston, MA, 2000.
[21] C.G. Christodoulou, M. Georgiopoulos, Application of Neural Networks in Electromagnetics, Artech House, MA, 2001.
[22] S.E. Fahlman, Fast learning variations on back propagation: an empirical study, in: D.S. Touretzky, G.E. Hinton, T.J. Sejnowski (Eds.), Proc. of the 1988 Connectionist Models Summer School, Morgan Kaufmann, San Mateo, CA, 1988, pp. 38–51.
[23] R.A. Jacobs, Increased rate of convergence through learning rate adaptation, Neural Networks 1 (1988) 295–307.
[24] A. Minai, R.D. Williams, Acceleration of back propagation through learning rate and momentum adaptation, in: Int. Joint Conf. on Neural Networks, January 01, 1990, pp. 676–679.
[25] A. López-Valdivieso, A. Robledo-Cabrera, A. Uribe-Salas, Flotation of celestite with the anionic collector sodium dodecyl sulfate. Effect of carbonate ions, Int. J. Miner. Process. 60 (2000) 79–90.
[26] J. Zhang, A.X. Wu, Y.M. Wang, X.S. Chen, Experimental research in leaching of copper-bearing tailings enhanced by ultrasonic treatment, J. China Univ. Min. Technol. 18 (2008) 0098–0102.

[27] Technical Publications Group, Neural Computing a Technology Handbook for Professional II/PLUS and Neuralworks Explorer, NeuralWare Inc., Pittsburgh, 1996.
[28] F. Pettersson, N. Chakraborti, H. Saxen, A genetic algorithms based multi-objective neural net applied to noisy blast furnace data, Appl. Soft Comput. 7 (2007) 387–397.
[29] F. Pettersson, A. Biswas, P.K. Sen, H. Saxen, N. Chakraborti, Analyzing leaching data for low-grade manganese ore using neural nets and multiobjective genetic algorithms, Mater. Manuf. Process 24 (2009) 320–330.
[30] G.J. Annandale, L. Lorenzen, J.S.J. VanDeventer, C. Aldrich, Neural net analysis of the liberation of gold using diagnostic leaching data, Miner. Eng. 9 (1996) 195–213.
[31] S.C. Chelgani, E. Jorjani, Artificial neural network prediction of Al_2O_3 leaching recovery in the Bayer process-Jajarm alumina plant (Iran), Hydrometallurgy 97 (2009) 105–110.
[32] A. Biswas, N. Chakraborti, P.K. Sen, A genetic algorithms based multi-objective optimization approach applied to a hydrometallurgical circuit for ocean nodules, Miner. Process. Extract. Metall. Rev. 30 (2009) 163–189.
[33] A. Biswas, N. Chakraborti, P.K. Sen, Multiobjective optimization of manganese recovery from sea nodules using genetic algorithms, Mater. Manuf. Process 24 (2009) 22–30.